Germanium- and Silicon-Substituted Donor–Acceptor Type Copolymers: Effect of the Bridging Heteroatom on Molecular Packing and Photovoltaic Device Performance

Jong Soo Kim, Zhuping Fei, Sebastian Wood, David T. James, Myungsun Sim, Kilwon Cho, Martin J. Heeney, and Ji-Seon Kim**

The effects of heteroatom substitution from a silicon atom to a germanium atom in donor-acceptor type low band gap copolymers, poly[(4,4′-bis(2-ethylhexyl)dithieno[3,2-b:2′,3′-d]silole)-2,6-diyl-alt-(2,1,3-benzothiadiazole)-4,7-diyl] (PSiBTBT) and poly[(4,4′-bis(2-ethylhexyl)dithieno[3,2-b:2′,3′-d]germole)-2,6-diyl-alt-(2,1,3-benzothiadiazole)-4,7-diyl] (PGeBTBT), are studied. The optoelectronic and charge transport properties of these polymers are investigated with a particular focus on their use for organic photovoltaic (OPV) devices in blends with phenyl-C_{70}-butyric acid methyl ester ($PC_{70}BM$). It is found that the longer C-Ge bond length, in comparison to C-Si, modifies the molecular conformation and leads to a more planar chain conformation in PGeBTBT than PSiBTBT. This increase in molecular planarity leads to enhanced crystallinity and an increased preference for a face-on backbone orientation, thus leading to higher charge carrier mobility in the diode configuration. These results provide important insight into the impact of the heavy atom substitution on the molecular packing and device performance of polymers based on the poly[2,6-(4,4-bis-(2-ethylhexyl)-4H-cyclopenta[2,1-b;3,4-b]-dithiophene)-alt-4,7-(2,1,3-benzothiadiazole) (PCPDTBT) backbone.

1. Introduction

The power conversion efficiency (PCE) of organic photovoltaic devices (OPV) based upon solution processed blends of conjugated donor polymers and small molecule acceptors has exceeded 9% [1] and significant efforts are now focused upon the fabrication of large area devices with regard to the commercialization of the technology.[2,3] In order to facilitate the move from small to large area devices it is important that the mechanisms governing charge generation and cell operation are well understood. In particular, the influence of blend morphology upon device performance is known to be critical, and therefore understanding the relationship between molecular structure and blend morphology is a crucial step towards controlling the microstructure. A particularly successful approach to the design of new, higher efficiency donor polymers has been the donor–acceptor approach, in which electron rich donor monomers are co-polymerized with electron deficient aromatics.[4,5] This has been demonstrated to lead to low optical band gaps by hybridization of the molecular orbitals.

Within the class of donor-acceptor polymers, bridged bithiophenes with five-member fused rings in the central core have proven to be a promising class of donor. The bridging atom keeps the bithiophene highly co-planar ensuring effective overlap of the conjugated systems, and additionally serves as a point of attachment for the required solubilizing groups. One such example polymer is poly[2,6-(4,4-bis-(2-ethylhexyl)-4H-cyclopenta[2,1-b;3,4-b]-dithiophene)-alt-4,7-(2,1,3-benzothiadiazole) (PCPDTBT), in which the bithiophene donor (cyclopentadithiophene, CPT) is bridged by a carbon atom.[6–8] Blends of PCPDTBT with [6,6]-phenyl C_{70} butyric acid methyl ester ($PC_{70}BM$) have reached a PCE around 5%. Since this initial promising solar cell performance of PCPDTBT blends, various approaches have been undertaken to further improve the efficiency. One interesting approach was to substitute the bridging C atom of CPT with different group IV heteroatoms. For example the analogous polymer incorporating a bridging silicon (Si) atom, poly[(4,4′-bis(2-ethylhexyl)dithieno[3,2-b:2′,3′-d]silole)-2,6-diyl-alt-(2,1,3-benzothiadiazole)-4,7-diyl] (PSiBTBT, **Scheme 1**a) showed an enhanced OPV device performance upon thermal treatment (unlike PCPDTBT) which was attributed to higher crystallinity of the Si based polymer.[9] The enhanced crystallinity of PSiBTBT over PCPDTBT has been associated with the C-Si bond being longer than the C-C bond of the central bridging five-membered ring, which changes the geometry of the fused

Dr. J. S. Kim, S. Wood, D. T. James, Dr. J.-S. Kim
Department of Physics & Centre for Plastic Electronics
Imperial College London
London SW7 2AZ, UK
E-mail: ji-seon.kim@imperial.ac.uk
Dr. Z. Fei, Dr. M. Heeney
Department of Chemistry & Centre for Plastic Electronics
Imperial College London
London SW7 2AZ, UK
E-mail: m.heeney@imperial.ac.uk
M. Sim, Prof. K. Cho
Department of Chemical Engineering
POSTECH, Pohang 790–784, South Korea

DOI: 10.1002/aenm.201400527

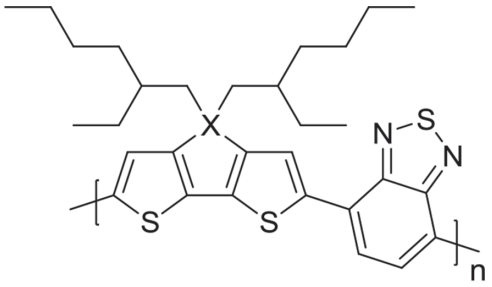

PCPDTBT X = C
PSiBTBT X= Si
PGeBTBT X=Ge

Scheme 1. Chemical structures of the polymers: a) poly[2,6-(4,4-bis-(2-ethylhexyl)-4H-cyclopenta[2,1-b;3,4-b]-dithiophene)-alt-4,7-(2,1,3-benzothiadiazole) (PCPDTBT), b) poly[(4,4′-bis(2-ethylhexyl) dithieno[3,2-b:2′,3′-d]silole)-2,6-diyl-alt-(2,1,3-benzothiadiazole)-4,7-diyl] (PSiBTBT), and c) poly[(4,4′-bis(2-ethylhexyl)dithieno[3,2-b:2′,3′-d]germole)-2,6- diyl-alt-(2,1,3-benzothiadiazole)-4,7-diyl] (PGeBTBT).

ring and facilitates interchain packing.[10,11] Furthermore, the bridging Si heteroatom can also affect the electronic properties of the polymer backbone, principally by interaction of the low lying σ^* orbital of the Si with the π^* orbitals of the conjugated system, resulting in the stabilization of the polymer LUMO level and narrowing the band gap.[12] These advantages were extended to germanium (Ge) bridged bithiophenes by several groups.[13–15] By substituting the bridging carbon atom in PCPDTBT with Ge, the analogous Ge substituted polymer poly[(4,4′-bis(2-ethylhexyl)dithieno[3,2-b:2′,3′-d]germole)-2,6-diyl-alt-(2,1,3-benzothiadiazole)-4,7-diyl] (PGeBTBT, Scheme 1b) was demonstrated to exhibit a reduced optical band gap.[13,14,16,17] We also found that the incorporation of the bridging Ge atom resulted in much higher stability to aqueous base than the Si analogue.[13] This was important because we were able to produce highly purified monomers which afforded high molecular weight polymer by a Suzuki cross-coupling procedure. In the case of the dithienosilole, the polymer is synthesized by a Stille cross-coupling and achieving the necessary high monomer purity required for high polymeric molecular weight is more challenging due to the poor stability of the organostannane monomer. Using the high molecular weight polymer, we reported very high photocurrents of ≈18 mA cm^{-2} under 1 Sun (AM 1.5) with 1:1 PGeBTBT/$PC_{70}BM$ blends. An overall PCE of 4.5% was achieved by adding solvent additives (1-chloronaphthalene, CN) and a post deposition thermal treatment. Our preliminary report indicated that PGeBTBT displayed semicrystalline behavior in pristine (i.e., non-blended) films, similar to PSiBTBT.[13]

By comparing PSiBTBT with PGeBTBT of similar molecular weight, we systematically explore the effects of heteroatom substitution from Si to Ge atom in these low band gap copolymers. With the detailed experimental (light absorption, crystalline packing- X-ray diffraction (XRD) and Raman spectroscopy) and quantum chemical simulation (torsion angle, bond length and calculated vibrational Raman spectrum), we clarify the influence of the heteroatom on the polymer backbone and correlate it to the bulk heterojunction OPV device performance. We find that the heavy atom affects the bond lengths and polymer backbone planarity, with a clear impact on the quality and orientation of molecular packing. In particular, PGeBTBT has a highly planar backbone leading to increased polymer film crystallinity and a preference for face-on backbone orientation. These factors lead to a high charge carrier mobility and photocurrent generation in photovoltaic devices.

2. Results and Discussion

The two polymers were prepared and purified as previously reported (see Supporting Information).[9,13] The molecular weights (M_n) measured by gel permeation chromatography in chlorobenzene at 80 °C were 19 kDa with a polydispersity (PD) of 2.05 for PSiBTBT and M_n 25 kDa (PD 3) for PGeBTBT against polystyrene standards. These correspond to degrees of polymerization of 35 and 42, respectively. The molecular weight of PSiBTBT is similar to that previously reported to give promising device performance.[9]

First, the optical properties of PSiBTBT and PGeBTBT solutions and thin films were investigated. Both polymers display qualitatively similar spectra, both in solution and thin film (**Figure 1**a, with a broad double peaked absorption in the long wavelength region 650–800 nm, and a less intense high energy absorption around 420 nm. The long wavelength absorption in donor-acceptor type copolymers is typically associated with an intramolecular charge transfer (ICT) transition from the donor to the acceptor, whilst the longer wavelength shoulder is associated with intermolecular aggregation.[18,19] As previously noted, PGeBTBT has a red shifted absorption compared to PSiBTBT with the first absorption peak at 773 nm compared to 751 nm in the thin film, which is indicative of increased backbone planarity.[5] In solution, the ratio of the lowest energy absorption peak (754 and 773 nm in PSiBTBT and PGeBTBT, respectively) to the second peak (692 and 695 nm in PSiBTBT and PGeBTBT respectively) within the first absorption band is also higher for the PGeBTBT with a value of 1.10 ± 0.01 compared to 0.94 ± 0.01. The origin of this lower energy peak is connected with polymer aggregation, which is confirmed by monitoring the optical absorption in the solution as a function of temperature, shown in Figure 1b. Upon heating, the lower energy peak decreases relative to the higher energy peak for both polymers i.e., reducing intermolecular interactions. The stronger absorption of this lower energy peak for PGeBTBT relative to PSiBTBT is indicative of more effective formation of polymer aggregates both in solution and in the solid state of PGeBTBT.

The optical absorption of the blend films of PGeBTBT with $PC_{70}BM$ is similar to the pristine polymer but with additional higher-energy (<650 nm) absorption from the $PC_{70}BM$. The blend films are spin-coated from the solutions with mixed solvents of chlorobenzene (CB) and chloronapthalene (CN) (used for optimized device performance). Comparing the absorption spectra of the blend films, it is apparent that the ratio of the lower energy aggregation peak to the higher energy second peak is reduced more strongly for PSiBTBT (1.01 to 0.93 ± 0.01) than for PGeBTBT (1.21 to 1.18 ± 0.01). This suggests that the addition of the fullerene is more disruptive to the ordering of the PSiBTBT polymer than the germanium analogue. The same trend is maintained after thermal annealing at 140 °C.

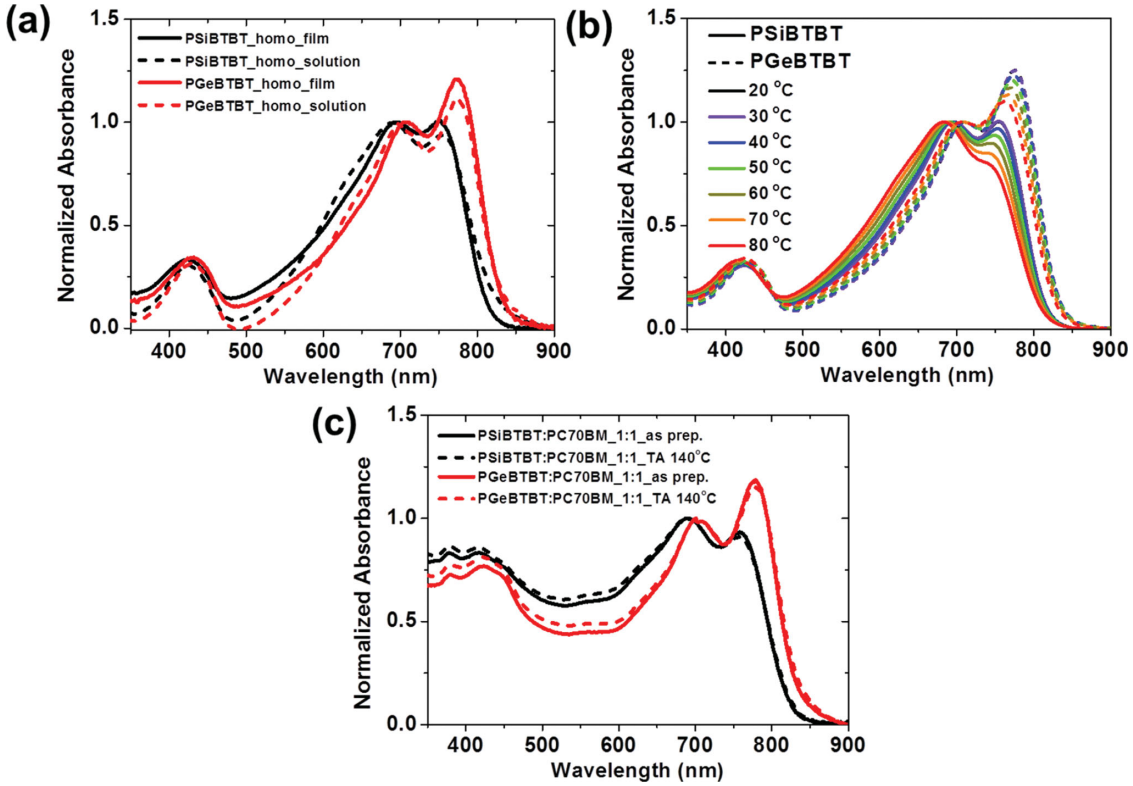

Figure 1. UV–vis spectra of the a) neat PSiBTBT and PGeBTBT film and solution of mixed solvent (CB + CN), b) temperature-dependent light absorption of PSiBTBT and PGeBTBT solutions, and c) PSiBTBT/PGeBTBT:$PC_{70}BM$ blend film spin coated by the CB + CN mixed solution with and without thermal treatment.

Photovoltaic performance (current density vs voltage) characteristics of these blend devices are shown in **Figure 2**a and **Table 1**. The indium tin oxide (ITO)/poly(3,4-ethylenedioxythiophene):polystyrene sulfonate (PEDOT:PSS)/polymer:$PC_{70}BM$/Ca/Al device configurations, in which the active layer was a 1:1 blend by weight in CB + CN solution, were compared after thermal annealing at 140 °C for 20 min. Device fabrication conditions were optimized by varying the solvent, additives, composition ratio and thermal annealing conditions (see Supporting Information for details). In both PSiBTBT and PGeBTBT blend devices, the overall PCE and fill factors (FF) are similar (4.23% vs 4.56% and 0.47 vs 0.43 for PSiBTBT:$PC_{70}BM$ and PGeBTBT:$PC_{70}BM$ respectively). However the open-circuit voltage (V_{oc}) and short-circuit current (J_{sc}) show clear differences. The PSiBTBT:$PC_{70}BM$ device has higher V_{oc} than that of PGeBTBT:$PC_{70}BM$ (0.65 V compared to 0.56 V) while J_{sc} is higher for PGeBTBT devices than PSiBTBT (18.6 mA cm^{-2} and 13.9 mA cm^{-2}, respectively). The increased V_{oc} for PSiBTBT in the blend devices with $PC_{70}BM$ is expected to result from a deeper highest occupied molecular orbital (HOMO) level.[20] On the other hand, the increase in the photocurrent (J_{sc}) in the PGeBTBT:$PC_{70}BM$ device can be understood by the significantly red-shifted absorption of PGeBTBT compared with PSiBTBT, which increases light harvesting of longer wavelength photons. As expected, the external quantum efficiency (EQE) as a function of excitation wavelength of these blend devices (Figure 2b) shows much higher EQE at wavelengths greater than 800 nm for the PGeBTBT:$PC_{70}BM$ blend demonstrating strongly enhanced photocurrent generation. We note that the performance of PSiBTBT in our work is similar to that previously reported in terms of V_{oc} and J_{sc}, with slightly lower FF.[9,21]

The measured photocurrent is also strongly dependent on the efficiency of charge transport and charge extraction from the device. The charge carrier mobilities of the PSiBTBT:$PC_{70}BM$ and PGeBTBT:$PC_{70}BM$ blends are compared using the space-charge limited current (SCLC) method for single carrier devices (Figure 2c).[22,23] Dark current density (J) vs voltage (V) characteristics of ITO/PEDOT:PSS/polymer:$PC_{70}BM$ (≈100 nm)/Au hole-only devices were measured to compare hole mobilities in these blend systems. The hole mobility values extracted using the modified Mott-Gurney equation are summarized in Table 1. The trend observed in hole mobilities in blend devices measured using this method is in good agreement with the trend observed in total J_{sc} values; i.e., PGeBTBT blend device (5.1×10^{-5} cm^2 V^{-1} s^{-1}) shows one order of magnitude higher hole mobility than PSiBTBT blend device (4.3×10^{-6} cm^2 V^{-1} s^{-1}). Therefore, we consider that the increase in photocurrent density in the PGeBTBT blend device, results from both the enhanced hole mobility and the enhanced optical absorption.

Now, we investigate the relationship between the molecular packing in PSiBTBT and PGeBTBT polymers on charge carrier mobilities and PV device performance. For this, we first compared the crystallinity of the polymers in neat and blend films using the grazing incidence X-ray diffraction (GI-XRD) technique. For the measurements, films were prepared under analogous conditions to the OPV devices. We compared the

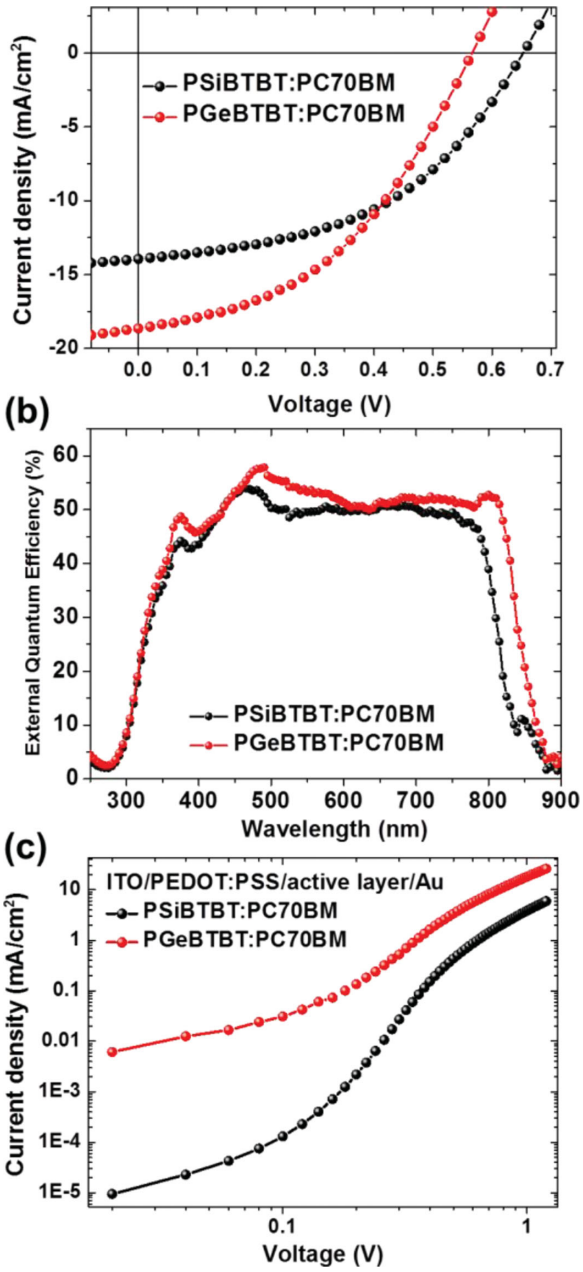

Figure 2. a) The representative current–voltage characteristics of OPV devices composed of PSiBTBT/PGeBTBT:$PC_{70}BM$ blend film, b) EQE data for PSiBTBT/PGeBTBT:$PC_{70}BM$ blend films and c) dark current density–voltage characteristics of PSiBTBT/PGeBTBT:$PC_{70}BM$ blend hole-only devices.

Table 1. Photovoltaic properties and hole mobilities measured in hole-only devices of polymers (PSiBTBT, PGeBTBT):PC70BM (1:1 by weight) blends (average values).

	V_{oc} [V]	J_{sc} [mA cm^{-2}]	FF	PCE [%]	Mobility from hole only devices [cm^2 V^{-1} s^{-1}]
PSiBTBT:$PC_{70}BM$	0.65	13.94	0.47	4.23	4.3×10^{-6}
PGeBTBT:$PC_{70}BM$	0.56	18.64	0.43	4.56	5.1×10^{-5}

neat and blend films with the same thickness of 110 nm by 2D (**Figure 3**a–d) and 1D (Figure 3e,f) XRD configurations.

In the out-of-plane direction, both films of PGeBTBT and PSiBTBT show a strong diffraction peak near $2\theta = 5°$, corresponding to a d-spacing of 16.6 Å for both PGeBTBT and PSiBTBT which originates from the interchain (100 plane) packing distance between polymer backbones. After blending with $PC_{70}BM$, the lattice spacing of the polymer backbone in the out-of-plane direction increases to 16.8 and 17.2 Å for PSiBTBT and PGeBTBT respectively. This widening of d-spacing suggests that the $PC_{70}BM$ molecules accumulate between the PGeBTBT polymer lamellae. The peak intensity of this (100) region is slightly higher for PSiBTBT in neat films, but similar in blend films. This indicates that both PSiBTBT and PGeBTBT polymers have a similar level of out-of-plane direction crystallinity in blends. On the other hand, in the (010) plane direction, PGeBTBT polymer shows much higher diffraction intensity than PSiBTBT polymer. A similar, much higher, (010) peak intensity is also observed in the PGeBTBT blend films. A more intense (010) plane peak indicates that the PGeBTBT polymer backbones have a more face-on configuration with in-plane stacking normal to the surface of the Si substrate. Note that in the PV device geometry where charge carriers are travelling in the vertical direction between the two electrodes, the π–π stacking direction of the polymer chains in (010) plane is critical for efficient charge collection. Therefore, the higher hole mobility observed in the PGeBTBT:$PC_{70}BM$ hole-only diodes (Figure 2c) can be explained by the preferential face-on packing of the PGeBTBT polymer relative to the PSiBTBT polymer.

Based on the XRD results, it is clear that the substitution of a bridging heteroatom in this donor-acceptor copolymer strongly influences the packing structure of polymer chains. The thin film crystallinity induced by improved polymer chain packing is enhanced in a particular direction, i.e., better packing in (010) plane direction for Ge atom compared to Si atom substitution. Note that no measurable crystallinity was observed in the C-based polymer (PCPDTBT) in neat films even with CN additives.[6] The reason for the PGeBTBT polymer preferring (010) plane stacking rather than (100) compared to PSiBTBT polymer is not clear, but we speculate that a higher degree of backbone planarity (see results below) in PGeBTBT may lead to the preferential face-on orientation. This is consistent with recent work by Chen et al. considering a different conjugated polymer series.[24]

Next, resonant Raman spectra of the polymer films were measured under 488 nm excitation in order to understand the crystallinity enhancement in PGeBTBT over PSiBTBT at a molecular scale. The strong Raman modes observed in the 1100–1600 cm^{-1} region (**Figure 4**) correspond with vibrations related to the conjugated backbone of the polymer, and these are typically sensitive to small differences in molecular structure and conformation.[25–27] The two polymer samples have comparable Raman spectra with similar mode frequencies and intensities, but there are some clear differences: the small mode visible at 1445 cm^{-1} for PSiBTBT is missing in PGeBTBT; the 1359 cm^{-1} mode in PSiBTBT shifts to 1367 cm^{-1} in PGeBTBT; the 1376 cm^{-1} mode in PSiBTBT shifts to 1381 cm^{-1} in PGeBTBT; and the relative intensities of the modes vary too. To understand these differences, the Raman active modes

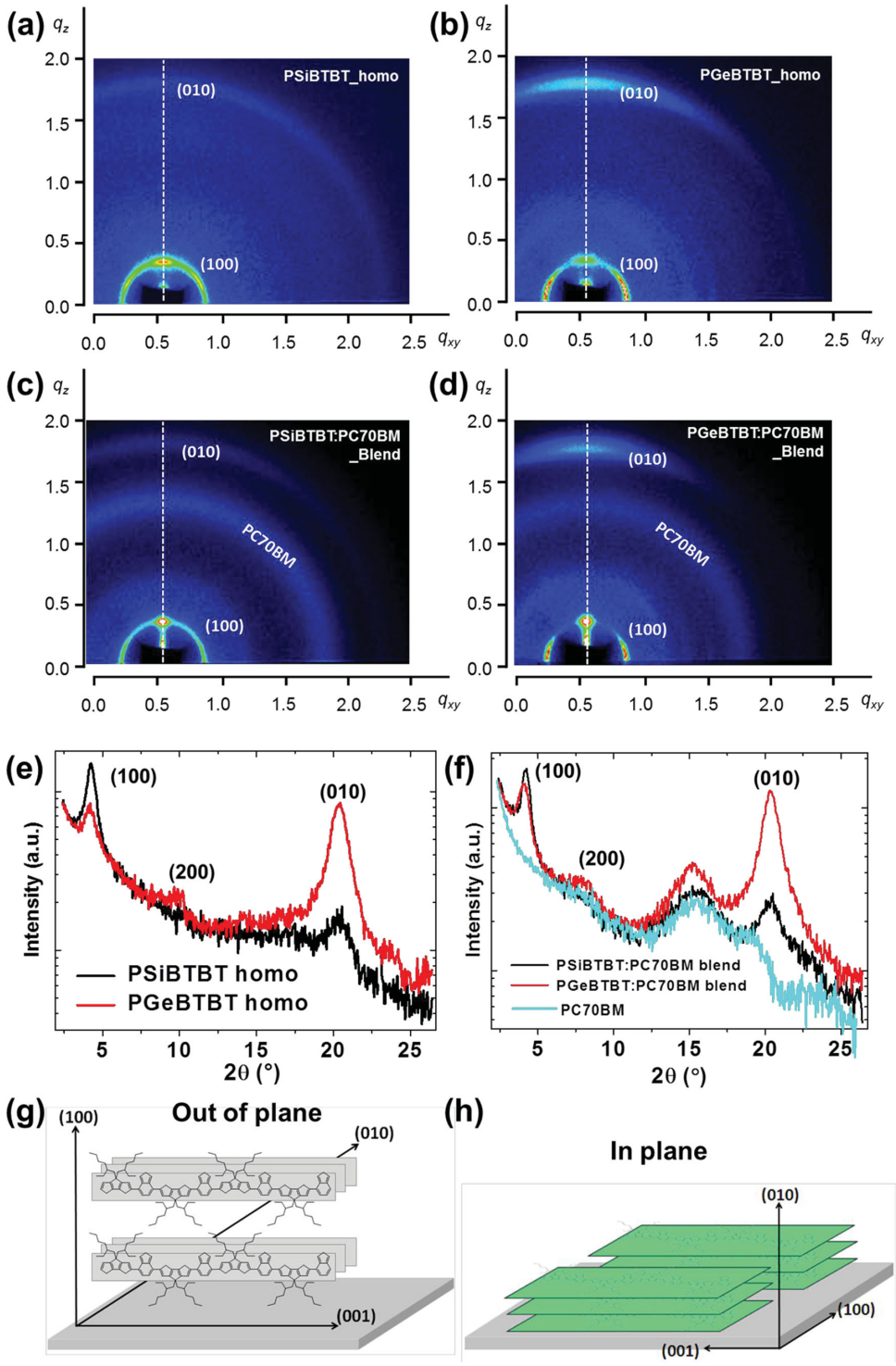

Figure 3. GI-XRD 2D data for a) PSiBTBT and b) PGeBTBT homo films, and c) PSiBTBT:$PC_{70}BM$ and d) PGeBTBT:$PC_{70}BM$ blend films. 1D GI-XRD data of e) PSiBTBT and PGeBTBT homo films, and f) PSiBTBT:$PC_{70}BM$ and PGeBTBT:$PC_{70}BM$ blend films. Diagrams illustrating out of plane (g) and in plane (h) packing structures.

were identified using a density functional theory (DFT) simulation of a segment of the conjugated backbone (see Supporting Information for details of mode assignment). We assign the 1530–1533 cm^{-1} mode to a ring stretch of the benzothiadiazole (BT) unit; the 1445 and 1469 cm^{-1} modes as C=C stretches of the fused thiophene ring (T) in the cyclopentadithiophene (CPT) unit; and the three main modes in the 1330–1410 cm^{-1} region are all C-C stretches along the conjugated backbone

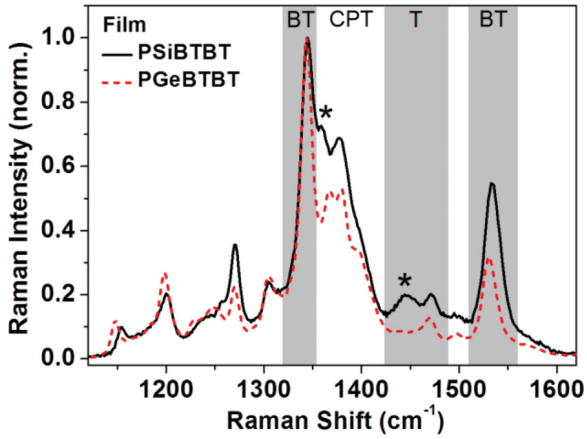

Figure 4. Raman spectra of PSiBTBT, and PGeBTBT thin films measured under 488 nm excitation, normalized to the 1345 cm^{-1} peak, showing assignment of peaks to benzothiadiazole (BT), cyclopendadithiophene (CPT) units, and the fused thiophene ring (T). Asterisks highlight significant peaks discussed in this work.

but with different degrees of localization on particular units. The 1345 cm^{-1} mode is localized mainly on the BT unit, the 1359–1367 cm^{-1} mode is more delocalized showing strong components on both the BT and the CPT units, whereas the 1376–1381 cm^{-1} mode is localized on the CPT unit.

These identifications enable an interpretation of the differences in the measured resonant Raman spectra of the two polymers in terms of their conformational changes. The 1445 and 1469 cm^{-1} modes visible in the PSiBTBT spectrum are two different vibrational modes associated with stretches of the C=C bonds in the fused thiophene ring (*c* and *d* in **Figure 5**). The DFT simulation only predicts one mode in this region (1469 cm^{-1}) but other published Raman spectra for thiophene-containing molecules show a range of thiophene C=C stretching mode energies so we suggest that the second peak (1445 cm^{-1}) is also associated with this part of the molecule.[28,29] The presence of these two modes indicates that there are two vibrational frequencies associated with these bonds – this agrees with the DFT geometry optimization, which gives different bond lengths (and hence difference force constants) for the two C=C bonds in the thiophene ring (*c* = 1.395 and *d* = 1.390 Å). The calculated lengths of these bonds for PGeBTBT are nearly equal (*c* = 1.392 and *d* = 1.390 Å), which provides an explanation for the absence of the lower energy (1445 cm^{-1}) Raman peak. The bond

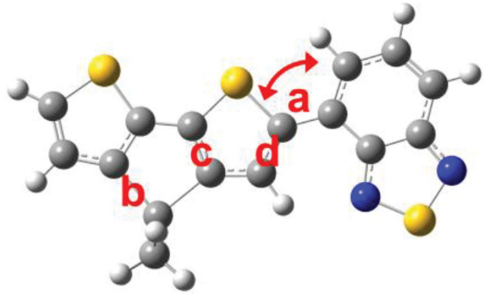

Figure 5. General molecular structure identifying bonds (*a*–*d*) discussed in the text.

which shows this difference in length (*c* in Figure 5) is the C=C bond shared by both the thiophene and the substituted cyclopentane ring and so we attribute the difference in PSiBTBT and PGeBTBT to an effect of the silicon/germanium substitution. The observed shifts in the 1359–1368 cm^{-1} and 1376–1381 cm^{-1} modes to higher energy in PGeBTBT are also attributed to structural changes. It is notable that the 1345 cm^{-1} peak position does not change, this is understandable since this mode is localized on the benzothiadiazole unit and so is far away from the substitution position, whereas the other two main backbone C-C modes have components on the cyclopentadithiophene unit. The shift to higher energies with the germanium substitution indicates a general reduction in the lengths of the C-C bonds within the cyclopentadithiophene unit compared with the silicon case.

In addition, the DFT geometry optimization shows a small reduction in inter-unit torsion (*a* in Figure 5) for PGeBTBT relative to PSiBTBT (0.16° and 0.75° respectively). The calculation also shows that the heteroatom substitution causes an increase in the C-X bond length (*b* in Figure 5) from C-C, through C-Si, to C-Ge (1.53, 1.89, and 1.95 Å), which is a likely cause for the structural changes described above.[10] The resonant Raman spectra provide experimental support for these molecular geometry calculations, and the XRD results clearly show the effect of these changes on long-range molecular order. The enhanced molecular packing and increased preference for a face-on polymer orientation in the germanium-substituted case can be attributed to the increased planarity of the polymer backbone. We suggest that this planarizing effect originates from the increased C-Ge bond length, which pushes the alkyl side chains further away from the conjugated backbone. These morphological changes correlate with improved charge carrier mobility and increased photocurrent generation.

3. Conclusion

In conclusion, narrow band gap polymers containing a germanium or silicon bridging atom were synthesized based on the structure of PCPDTBT. The optoelectronic and charge transport properties were systematically investigated to elucidate the effect of this heavy atom substitution on bulk heterojunction photovoltaic devices using $PC_{70}BM$ as the electron acceptor. A complementary study of the molecular conformation and molecular packing using resonant Raman spectroscopy and 2D-XRD, supported by DFT calculations revealed that the germanium substitution (PGeBTBT) caused an increase in the C-Ge bond length and led to a more planar polymer backbone, which enhanced molecular packing with a face-on orientation. This resulted in an increased hole mobility and a high photocurrent density (18.6 mA cm^{-2}).

4. Experimental Section

The polymers studied in this work (PCPDTBT, PSiBTBT and PGeBTBT) were synthesized using the methods referred in the literature and $PC_{70}BM$ was purchased from Nano-C (used as received).[6–8,10,13] Organic photovoltaic devices were fabricated by blending PGeBTBT (PSiBTBT) with $PC_{70}BM$ as the electron donor and acceptor respectively. Devices were fabricated on indium tin oxide (ITO) coated substrates with the device structure ITO/PEDOT:PSS/PGeBTBT (PSiBTBT):$PC_{70}BM$/Ca/

Al. After sequential cleaning of the ITO with the detergent (Mucasol), acetone and isopropyl alcohol, poly(3,4-ethylenedioxythiophene)-poly(styrene sulfonate) (PEDOT:PSS, Baytron P TP AI 4083, Bayer AG) was spin coated onto the ITO substrate with a thickness of 30 nm and baked at 120 °C for 30 min. PGeBTBT (PSiBTBT):$PC_{70}BM$ solutions in chlorobenzene (CB) at different weight ratios were stirred overnight at 100 °C with or without a small amount of 1-chloronaphthalene (CN, 3%). The best device performance was obtained at the blend ratio of 1:1 solution (24 mg mL^{-1}) by spin coating onto the PEDOT:PSS coated ITO substrate (1500 rpm, 2 min) with a hot (100 °C) metal chuck. The thickness of the active layer was ≈120 nm. After spin coating the active layers, films were thermally annealed at 140 °C for 20 min. For the power conversion efficiency (PCE) measurement of OPV devices, we used thermally deposited Ca (20 nm)/Al (100 nm) cathodes. Electrical characteristics were measured by Keithley 236 source/measure unit under AM 1.5 solar illumination (Oriel 300 W solar simulator) at an intensity of 100 mW cm^{-2} with a device area of 0.045 cm^2. All electrical measurements of OPVs were executed in a N_2 purged device chamber. Hole-only devices were fabricated using PEDOT:PSS and Au electrodes to measure the hole mobilities of the blend films. We measured the external quantum efficiency as a function of excitation wavelength with a photomodulation spectroscopic setup. UV–vis absorption spectra were measured using an absorption spectrophotometer (UV 2500, Shimadzu). The thin film morphologies were characterized using the topography mode of an atomic force microscope (DI, Nanoscope VI). XRD measurements were performed at the grazing incidence XRD setup at the PAL (Pohang Accelerator Laboratory, 10C1 beam line) synchrotron. Raman spectra were recorded under a 488 nm excitation wavelength (0.01mW, acquisition time of 10~20s). The spectra were background corrected and averaged over measurements taken at three different regions. The spectra at the different regions were very similar indicating the reproducibility of the results. Quantum chemical calculations were performed with GAUSSIAN09 using DFT at the B3LYP level with the 6–31G(d) basis set and an empirical scaling factor for vibrational mode frequencies.[30–34]

Supporting Information

Supporting Information is available from the Wiley Online Library or form the author.

Acknowledgements

This work was supported by the EMRP-REG project (under JRP: IND07) and the EPSRC via SCALLOPS project (EP/J500021/1), SUPERGEN project (EP/G031088/1), research grant (EP/G060738/1) and Center for Doctoral Training (EP/G037515/1).

Received: March 28, 2014
Revised: June 21, 2014
Published online: July 29, 2014

[1] Z. He, C. Zhong, S. Su, M. Xu, H. Wu, Y. Cao, *Nat. Photonics* **2012**, *6*, 591.
[2] R. Po, A. Bernardi, A. Calabrese, C. Carbonera, G. Corso, A. Pellegrino, *Energy Environ. Sci.* **2014**, *7*, 925.
[3] M. Hösel, R. R. Søndergaard, D. Angmo, F. C. Krebs, *Adv. Eng. Mater.* **2013**, *15*, 995.
[4] C.-P. Chen, S.-H. Chan, T.-C. Chao, C. Ting, B.-T. Ko, *J. Am. Chem. Soc.* **2008**, *130*, 12828.
[5] P. M. Oberhumer, Y.-S. Huang, S. Massip, D. T. James, G. Tu, S. Albert-Seifried, D. Beljonne, J. Cornil, J.-S. Kim, W. T. S. Huck, N. C. Greenham, J. M. Hodgkiss, R. H. Friend, *J. Chem. Phys.* **2011**, *134*, 114901.
[6] W. Ma, C. Yang, X. Gong, K. Lee, A. J. Heeger, *Adv. Funct. Mater.* **2005**, *15*, 1617.
[7] J. K. Lee, W. L. Ma, C. J. Brabec, J. Yuen, J. S. Moon, J. Y. Kim, K. Lee, G. C. Bazan, A. J. Heeger, *J. Am. Chem. Soc.* **2008**, *130*, 3619.
[8] J. Peet, N. S. Cho, S. K. Lee, G. C. Bazan, *Macromolecules* **2008**, *41*, 8655.
[9] J. Hou, H.-Y. Chen, S. Zhang, G. Li, Y. Yang, *J. Am. Chem. Soc.* **2008**, *130*, 16144.
[10] H.-Y. Chen, J. Hou, A. E. Hayden, H. Yang, K. N. Houk, Y. Yang, *Adv. Mater.* **2010**, *22*, 371.
[11] M. C. Scharber, M. Koppe, J. Gao, F. Cordella, M. A. Loi, P. Denk, M. Morana, H.-J. Egelhaaf, K. Forberich, G. Dennler, R. Gaudiana, D. Waller, Z. Zhu, X. Shi, C. J. Brabec, *Adv. Mater.* **2010**, *22*, 367.
[12] J. Ohshita, *Macromol. Chem. Phys.* **2009**, *210*, 1360.
[13] Z. Fei, J. S. Kim, J. Smith, E. B. Domingo, T. D. Anthopoulos, N. Stingelin, S. E. Watkins, J.-S. Kim, M. Heeney, *J. Mater. Chem.* **2011**, *21*, 16257.
[14] D. Gendron, P. Morin, P. Berrouard, N. Allard, B. R. Aïch, C. N. Garon, Y. Tao, M. Leclerc, *Macromolecules* **2011**, *44*, 7188.
[15] C. M. Amb, S. Chen, K. R. Graham, J. Subbiah, C. E. Small, F. So, J. R. Reynolds, *J. Am. Chem. Soc.* **2011**, *133*, 10062.
[16] J. Ohshita, Y. Hwang, T. Mizumo, H. Yoshida, Y. Ooyama, Y. Harima, Y. Kunugi, *Organometallics* **2011**, *30*, 3233.
[17] C. P. Yau, Z. Fei, R. S. Ashraf, M. Shahid, S. E. Watkins, P. Pattanasattayavong, T. D. Anthopoulos, V. G. Gregoriou, C. L. Chochos, M. Heeney, *Adv. Funct. Mater.* **2013**, DOI: 10.1002/adfm.201302270.
[18] K. G. Jespersen, W. J. D. Beenken, Y. Zaushitsyn, A. Yartsev, M. Andersson, T. Pullerits, V. Sundström, *J. Chem. Phys.* **2004**, *121*, 12613.
[19] R. Steyrleuthner, M. Schubert, I. Howard, B. Klaumünzer, K. Schilling, Z. Chen, P. Saalfrank, F. Laquai, A. Facchetti, D. Neher, *J. Am. Chem. Soc.* **2012**, *134*, 18303.
[20] B. C. J. Brabec, A. Cravino, D. Meissner, N. S. Sariciftci, T. Fromherz, M. T. Rispens, L. Sanchez, J. C. Hummelen, *Adv. Funct. Mater.* **2001**, 374.
[21] M. Morana, H. Azimi, G. Dennler, H.-J. Egelhaaf, M. Scharber, K. Forberich, J. Hauch, R. Gaudiana, D. Waller, Z. Zhu, K. Hingerl, S. S. van Bavel, J. Loos, C. J. Brabec, *Adv. Funct. Mater.* **2010**, *20*, 1180.
[22] V. D. Mihailetchi, H. X. Xie, B. de Boer, L. J. a. Koster, P. W. M. Blom, *Adv. Funct. Mater.* **2006**, *16*, 699.
[23] V. D. Mihailetchi, J. Wildeman, P. W. M. Blom, *Phys. Rev. Lett.* **2005**, *94*, 126602.
[24] M. S. Chen, J. R. Niskala, D. A. Unruh, C. K. Chu, O. P. Lee, J. M. J. Frechet, *Chem. Mater.* **2013**, *25*, 4088.
[25] S. Wood, J. S. Kim, D. T. James, W. C. Tsoi, C. E. Murphy, J.-S. Kim, *J. Chem. Phys.* **2013**, *139*, 064901.
[26] W. C. Tsoi, W. Zhang, J. Razzell Hollis, M. Suh, M. Heeney, I. McCulloch, J.-S. Kim, *Appl. Phys. Lett.* **2013**, *102*, 173302.
[27] W. C. Tsoi, D. T. James, E. B. Domingo, J. S. Kim, M. Al-Hashimi, C. E. Murphy, N. Stingelin, M. Heeney, J.-S. Kim, *ACS Nano* **2012**, *6*, 9646.
[28] J.-H. Kim, C. E. Song, N. Shin, H. Kang, S. Wood, I. Kang, B. J. Kim, B. Kim, J. Kim, W. S. Shin, D. Hwang, *ACS Appl. Mater. Interfaces* **2013**, *5*, 12820.
[29] W. C. Tsoi, D. T. James, J. S. Kim, P. G. Nicholson, C. E. Murphy, D. D. C. Bradley, J. Nelson, J.-S. Kim, *J. Am. Chem. Soc.* **2011**, *133*, 9834.
[30] M. J. Frisch, G. W. Trucks, H. B. Schlegel, G. E. Scuseria, M. A. Robb, J. R. Cheeseman, G. Scalmani, V. Barone, B. Mennucci, G. A. Petersson, H. Nakatsuji, M. Caricato, X. Li, H. P. Hratchian, A. F. Izmaylov, J. Bloino, G. Zheng, J. L. Sonnenberg, M. Hada, M. Ehara, K. Toyota, R. Fukuda, J. Hasegawa, M. Ishida, T. Nakajima, Y. Honda, O. Kitao, H. Nakai, T. Vreven,

J. A. Montgomery, Jr., J. E. Peralta, F. Ogliaro, M. Bearpark, J. J. Heyd, E. Brothers, K. N. Kudin, V. N. Staroverov, R. Kobayashi, J. Normand, K. Raghavachari, A. Rendell, J. C. Burant, S. S. Iyengar, J. Tomasi, M. Cossi, N. Rega, J. M. Millam, M. Klene, J. E. Knox, J. B. Cross, V. Bakken, C. Adamo, J. Jaramillo, R. Gomperts, R. E. Stratmann, O. Yazyev, A. J. Austin, R. Cammi, C. Pomelli, J. W. Ochterski, R. L. Martin, K. Morokuma, V. G. Zakrzewski, G. A. Voth, P. Salvador, J. J. Dannenberg, S. Dapprich, A. D. Daniels, Ö. Farkas, J. B. Foresman, J. V. Ortiz, J. Cioslowski, D. J. Fox, Gaussian 09, Revision A.1 **2009**.

[31] A. D. Becke, *J. Chem. Phys.* **1993**, *98*, 5648.

[32] C. Lee, W. Yang, R. G. Parr, *Phys. Rev. B* **1988**, *37*, 785.

[33] W. J. Hehre, R. Ditchfield, J. A. Pople, *J. Chem. Phys.* **1972**, *56*, 2257.

[34] K. K. Irikura, R. D. Johnson, R. N. Kacker, *J. Phys. Chem. A* **2005**, *109*, 8430.